PERGAMON

Progress in Biophysics & Molecular Biology 74 (2000) 63–91

Progress in Biophysics & Molecular Biology

www.elsevier.com/locate/pbiomolbio

Review

Mechanical design of proteins studied by single-molecule force spectroscopy and protein engineering

Mariano Carrion-Vazquez*, Andres F. Oberhauser, Thomas E. Fisher, Piotr E. Marszalek, Hongbin Li, Julio M. Fernandez

Department of Physiology and Biophysics, Mayo Foundation, 1-159 Medical Sciences Building, Rochester, MN 55905, USA

Abstract

Mechanical unfolding and refolding may regulate the molecular elasticity of modular proteins with mechanical functions. The development of the atomic force microscopy (AFM) has recently enabled the dynamic measurement of these processes at the single-molecule level. Protein engineering techniques allow the construction of homomeric polyproteins for the precise analysis of the mechanical unfolding of single domains. α-Helical domains are mechanically compliant, whereas β-sandwich domains, particularly those that resist unfolding with backbone hydrogen bonds between strands perpendicular to the applied force, are more stable and appear frequently in proteins subject to mechanical forces. The mechanical stability of a domain seems to be determined by its hydrogen bonding pattern and is correlated with its kinetic stability rather than its thermodynamic stability. Force spectroscopy using AFM promises to elucidate the dynamic mechanical properties of a wide variety of proteins at the single molecule level and provide an important complement to other structural and dynamic techniques (e.g., X-ray crystallography, NMR spectroscopy, patch-clamp).

Contents

*Corresponding author. Tel.: +1-507-284-9442; fax: +1-507-284-0521.
E-mail address: carrion.mariano@mayo.edu (M. Carrion-Vazquez).

0079-6107/00/$ - see front matter
PII: S0079-6107(00)00017-1

1. Introduction and overview

The importance of mechanical forces at the molecular level of biological systems has become increasingly apparent during the last few years (Bensimon, 1996; Evans and Ritchie, 1997; Erickson, 1994, 1997; Hynes, 1999; Chicurel et al., 1998; Ohashi et al., 1999; Shaub, 1999; Bustamente et al., 2000). Since many proteins are exposed to mechanical tension, a variety of topological solutions to use or resist force may have arisen through evolution. An example of a protein under mechanical tension is the muscle protein titin, which is responsible of the passive elasticity of muscle. Proteins from the extracellular matrix (ECM) and the cytoskeleton also operate under tension. Evidence from in vivo studies suggests that tension on the ECM protein fibronectin triggers domain unfolding exposing cryptic binding sites that are important for the ECM assembly (Ohashi et al., 1999). The physical properties underlying the mechanical functions of proteins are largely unknown, but one structural characteristic common to many proteins exposed to mechanical tension is that they contain multiple individually folded domains.

Atomic force microscopy (AFM) has been applied recently to the analysis, at the single-molecule level, of the mechanical properties of modular proteins with mechanical functions from muscle, ECM, and cytoskeleton. This has made it possible to examine the elastic properties of proteins composed of a variety of heterogeneous tandem modules, such as the immunoglobulin (Ig) and fibronectin type III (FN-III) domains of titin (Rief et al., 1997a, 1998), the FN-III domains of tenascin (Oberhauser et al., 1998), and the triple helical coiled-coils of spectrin (Rief et al., 1999).

The combination of protein engineering techniques with single-molecule AFM has recently allowed the study of the mechanical properties of single modules (Carrion-Vazquez et al., 1999a,b;

Yang et al., 2000). A prerequisite for these studies was the construction of identical tandem repeats of the domain under study. Recombinant DNA technology has made homomeric polyproteins available, which has opened the door to the analysis of the mechanical properties of individual modules. These techniques have built upon information derived from NMR spectroscopy and dynamic molecular simulations to identify the determinants of mechanical stability in an immunoglobulin domain from human cardiac titin. This combined approach allows us to examine the determinants of stability in different types of protein folds and to compare their mechanical properties.

Several reviews have recently appeared covering the emerging field of single-protein force spectroscopy by AFM (Engel et al., 1999; Ludwig et al., 1999; Fisher et al., 1999a,b; Fisher et al., 2000a,b; Strick et al., 2000; Janshoff et al., 2000). This review will outline the recent combination of AFM and molecular biology to study the molecular determinants of the mechanical stability of proteins. In particular, it will discuss the application of this approach to compare the mechanical stability of proteins that are α-helical to those that are β-barreled and to examine the mechanical properties of proteins that lack known mechanical function.

2. The mechanical unfolding of single proteins by AFM

In contrast to classical imaging instruments such as light and electron microscopes, scanning probe microscopes use a stylus to scan a sample surface and monitor a variety of interactions between the stylus tip and the sample. Since its invention in 1986 (Binnig et al., 1986), the AFM has been the most widely used scanning probe microscope for biological applications. The AFM is a remarkably simple instrument that works like a miniature phonograph and is capable of imaging single macromolecules with submolecular resolution (Bustamante et al., 1997; Czajkowsky and Shao, 1998). The ''force spectroscopy'' or ''force-measuring'' mode of the AFM was later developed to measure nanomechanical properties of materials (Burnham and Colton, 1989) and has allowed the measurement of the binding forces of complementary DNA strands (Lee et al., 1994) and receptor–ligand systems (Florin et al., 1994), as well as the forces that maintain the conformation of sugar rings in a polysaccharide (Rief et al., 1997b; Marszalek et al., 1998, 1999a) and folded domains in a modular protein (Rief et al., 1997a). This technique is capable of measuring the forces required to unfold protein domains with piconewton (pN) sensitivity and the length changes with Ångstrom resolution. In this configuration, a single protein is suspended between a sharp tip of silicon nitride, mounted on a cantilever, and a substrate mounted on a high precision piezoelectric positioner to allow control of its vertical movement. In a typical experiment (see Fig. 1), the tip of the cantilever is brought into contact with a layer of protein attached to the substrate, then the piezoelectric positioner retracts. When a portion of a single protein molecule is picked up at random by the tip through adsorption, the retraction of the positioner stretches the suspended segment of the protein. The first source of resistance to extension of the protein are entropic forces (like any other polymer, proteins tend to coil up to maximize the disorder of their constituent segments). Extension of the molecule reduces its entropy producing a restoring force that results in bending of the cantilever. This deflection changes the angle of reflection of a laser beam bounced off the surface of the cantilever and is measured as a change in output from a

photodetector. Using the spring constant of the cantilever, the relationship between deflection and force can be calibrated and the force calculated. The entropic elasticity of the protein can be formally described by the worm-like chain (WLC) model of polymer elasticity (Fig. 1). The additional extension of the protein may cause unraveling of the protein fold increasing the effective length of the polymer between the tip and the substrate and dropping the force acting on the cantilever to near zero.

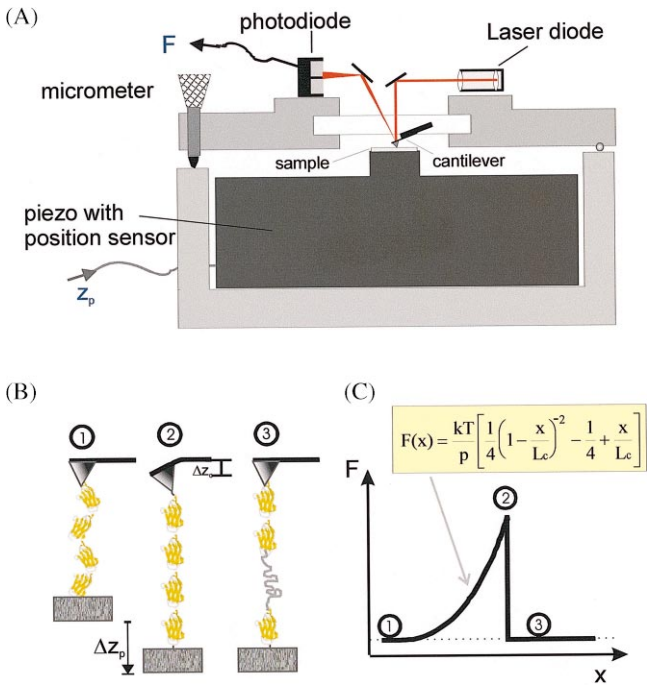

Fig. 1. Using the atomic force microscope to measure the molecular elasticity of single proteins. (A) A schematic of our custom-built AFM. The AFM uses a Digital Instruments AFM detector head mounted on top of a single-axis piezoelectric positioner from Physik Instrumente. The positioner has a capacitative sensor with a Z-axis resolution of 1 Å. Data acquisition and the voltage control of the piezoelectric positioner are achieved using a PC-mounted data acquisition board controlled by custom-made LabView (National Instruments) software. The force is measured by the deflection of the cantilever and the extension can be calculated from the position of the piezoelectric actuator (z_p). (B) The unfolding of a protein domain by an external force. When axial stress is applied to a folded domain the protein will unravel. As the distance between substrate and cantilever increases (from states 1 to 2) the protein elongates and the reduction of its entropy generates a restoring force that bends the cantilever. When a domain unfolds (state 3) the contour length of the protein increases, returning the force on the cantilever to near zero. Further extension again results in force on the cantilever (state 1 again). (C) The entropic elasticity of proteins can be described by the worm-like chain (WLC) model of polymer elasticity (inset). This equation predicts the entropic restoring force (F) generated upon extension (x) of a protein in terms of its persistence length (p) and its contour length (L_C) (Rief et al., 1997a; Marko and Siggia, 1995). In general, polymer elasticity results from the tendency of a chain to coil in order to maximize its conformational freedom (entropy) under the drive of thermal fluctuations. Extending a relaxed polymer chain generates an opposing force that is predicted from the reduction in the entropy of the polymer. This effect is known as entropic elasticity and is the basis of the elasticity of proteins. The saw-tooth pattern of peaks on the force-extension relationship corresponds to sequential unraveling of individual domains of a modular protein like the one shown here. The numbers correspond to the stages marked in 1(B).

Until recently, the only way to measure the stability of a protein was to change its physical (e.g., with heat or high pressure) or chemical environment (e.g., with guanidinium chloride or urea, acidic or alkaline pH) and monitor the loss of protein conformation, using spectroscopic techniques from which folding free energies could be obtained. However, the series of conformational changes that a protein undergoes in response to mechanical stress, as may occur in vivo, may be very different. AFM force spectroscopy offers several advantages over thermal or chemical denaturation. First of all, AFM allows the measurement of folding reactions at the single-molecule level and therefore can uncover rare unfolding events that are not observed by using traditional bulk methods, in which measured parameters are averaged over populations of many molecules. It acts directly on the protein molecule, leaving its environment untouched. It can increase the rate of unfolding exponentially, reducing considerably the experimental time. It allows a direct measurement of the mechanical stability of the fold. The process of mechanical unfolding is therefore defined as a function of extension (here the reaction coordinate is well defined, i.e. length), which in the case of proteins exposed to stress in vivo, may be a more physiological perturbation. In contrast to other structural techniques (i.e. X-ray crystallography), force spectroscopy is dynamic and it works in real time. Tiny amounts of protein are needed (typically a few μg), it is not limited to a range of molecular weights, and it works in aqueous solution, so crystal formation is not required.

3. The use of engineered polyproteins in force spectroscopy

3.1. The advantage of polyproteins for AFM studies

When a cantilever tip is pressed against a layer of protein and then withdrawn, many protein molecules attached to the substrate will interact with the tip and thus transmit a force that will bend the cantilever. Only rarely will the entire properly folded molecule of interest be suspended between substrate and tip. More commonly, the interaction will involve only a fragment of the protein, which may be in a denatured form. The consequences of such ''nonspecific'' interactions are illustrated in Fig. 2. The early part of the force–extension curve, which reflects the time during which the cantilever tip is close to the substrate, is typically characterized by large fluctuations in force. This poses two difficulties to the interpretation of AFM force–extension curves. First, the forces involved in extending short molecules may be masked by the ''noise'' caused by such nonspecific interactions. Second, since almost all recordings show force peaks reflecting such interactions between the cantilever tip and the adsorbed protein layer, a means is needed to differentiate true unfolding events from spurious interactions.

The problem of nonspecific interactions was surmounted in the pioneer AFM studies by the use of multidomain proteins. Thus, the presence of multiple Ig and FN-III domains in titin and tenascin enabled the detection of domain unfolding (Rief et al., 1997a; Oberhauser et al., 1998). However, modular proteins are constituted by heterogeneous populations of modules (differing in size, structure, sequence and stability) and it is not possible to identify the force peaks corresponding to the unfolding of specific domains. The construction of homomeric polyproteins (i.e., tandem repeats of a single domain) now allows the study of the mechanical properties of

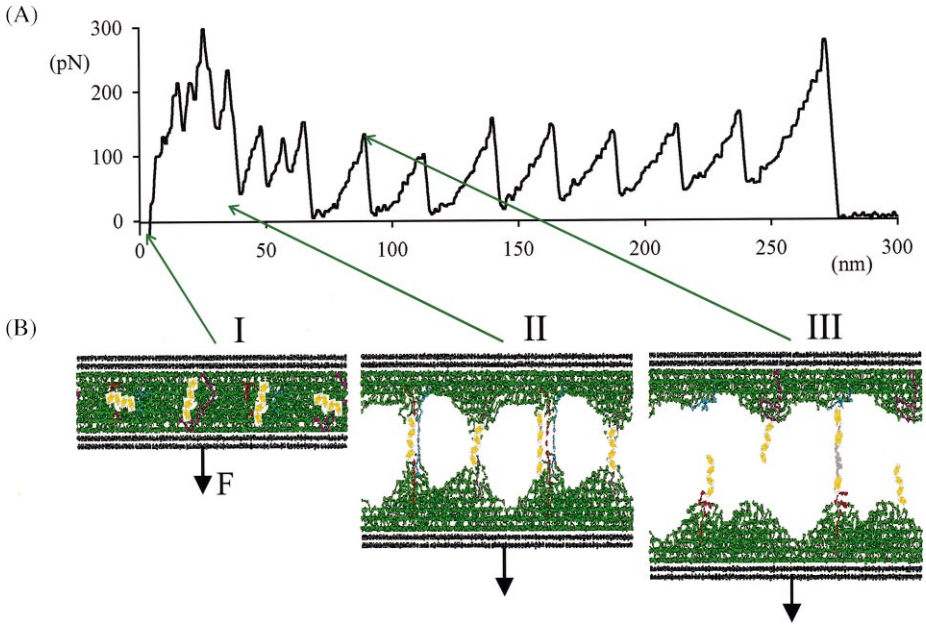

Fig. 2. (A) Force–extension recording of a single polyprotein measured with AFM techniques. A typical individual protein domain of 100 amino acids would have a folded length of 1.5 to 6 nm but an unfolded length of about 40 nm (length of an amino acid: 0.40 nm). In AFM, the first 30 to 75 nm are typically obscured by nonspecific interactions between the cantilever tip and the polyprotein layer. (B) A hypothetical series of events as an AFM tip is pressed against a monolayer of polymers and then withdrawn (modified from Baljon and Robbins, 1996). Colors represent different conformations of the same polyprotein, yellow being the native fold. Panel I shows the compression of the protein layer as the tip is pressed against it. As the substrate is withdrawn (panel II) some of the molecules are adsorbed to the tip. The bonds between the two layers are gradually broken until a single protein forms the only connection between the two surfaces. On further extension, the independent domains of the protein begin to unfold (panel III).

specific domains (Carrion-Vazquez et al., 1999a). Unlike native modular proteins, polyproteins have a perfect repetitive structure that results in a unique periodical saw-tooth pattern in force-extension recordings. This ''fingerprint'' clearly demonstrates that domains from a single molecule are being unfolded and enables the measurement of the force required to unfold those domains as well as their size.

Studies with the I27 module of human cardiac titin (see below) have shown several more advantages of polyproteins in force spectroscopy. As we shall see in Section 5.1.1, polyproteins produce a linear increase of the spatial resolution which is positively correlated with the increasing number of modules in the polyprotein (i.e., there is an increase of the signal-to-noise ratio). The use of this ''amplification'' by repetition of protein modules allows amino acid resolution to be easily obtained in force–extension recordings and enables accurate module sizing of both the folded and unfolded domains (Carrion-Vazquez et al., 1999b). This amplification by polyproteins has also uncovered subtle folding intermediates in the mechanical unfolding of Ig domains from titin (Marszalek et al., 1999b).

3.2. Periodic patterns of force peaks measured by AFM represent true unfolding events

Proteins tend to denature to some extent when adsorbed onto a surface (Buijs et al., 1996; Hlady and Buijs, 1998). Therefore, it is important to demonstrate that the patterns observed with AFM correspond to true unfolding events rather than to the detachment of denatured proteins adsorbed onto a surface. With the use of polyproteins in force spectroscopy, a body of experimental evidence has accumulated that refutes protein desorption as an explanation for the force–extension curves observed. The following is a list of these arguments (many of which are based on observations described in Section 5.1.1):

(1) The rate of module unfolding of I27 measured by AFM ($3.3 \times 10^{-4}\,s^{-1}$) is comparable to that obtained from chemical denaturation experiments ($4.9 \times 10^{-4}\,s^{-1}$) (Carrion-Vazquez et al., 1999a). Similar results are obtained using poly-I28, which has also comparable mechanical ($2.8 \times 10^{-5}\,s^{-1}$) and chemical ($1.6 \times 10^{-5}\,s^{-1}$) unfolding rates (Li et al., 2000). These similarities would be difficult to explain using a disorption model and provide strong evidence that saw-tooth patterns represent true protein unfolding events.

(2) When a polyprotein is stretched by AFM, the interval between peaks is highly reproducible and corresponds closely to that expected based on NMR and molecular dynamics simulations. In the case of the I27 module from human cardiac titin (see Section 5.1.1 for details) the folded core encompasses about 72 amino acids (there is uncertainty about its boundaries) and the observed distance between peaks (28.1 ± 0.17 nm) corresponds to 70 amino acids, considering that, as we shall see in Section 5.1.1.5., the length of each amino acid residue is 0.40 nm ($70 \times 0.40\,nm \approx 28.1\,nm$). Since the I27 domain has a total of 89 amino acids, these results imply that the "spacer sequence" between the folded cores of the polyprotein is fully extended prior to the unraveling events. This is inconsistent with a desorption hypothesis, which would predict equal intervals corresponding to the full folded length of each domain or an alternating pattern of two different intervals corresponding to two elements in series ("spacers" and "folded core"). Furthermore, when insertions of 5 glycine residues where made inside the folded core the spacing between peaks increased by the expected distance; similar insertions made outside of this region did not change the intervals (Carrion-Vazquez et al., 1999b). These experiments confirm that the spacer regions are extended prior to unfolding.

(3) Force–extension recordings of a $(I27–I28)_4$ heterodimeric polyprotein (constructed out of 4 repeats of a I27–I28 dimer) show saw-tooth patterns with force peaks clustered into two classes, the first 4 peaks being ~200 pN and the remaining 4 peaks being ~300 pN (pulling speed: 0.6 nm/ms). The force of unfolding of I27 and I28 homomeric polyproteins suggests that the weaker peaks represent unfolding of I27 domains while the stronger ones represent unfolding of I28 modules. If the force peaks were due to sequential desorption of the modules an alternating pattern of force peaks would be expected for this construct, according with its linear arrangement (Fig. 3; Li et al., 2000).

(4) When titin modules are stretched, the force peaks of the force–extension curves tend to be ordered from weakest to strongest (Rief et al., 1997a). This suggests that in the protein modules are unfolding in an order according to their mechanical stability rather than desorbing in a linear fashion from the point of pulling.

(5) Additional evidence that favors the unfolding model comes from the fact that the forces (pulling speed: 0.6 nm/ms) and the spacing between peaks are distant and different for different

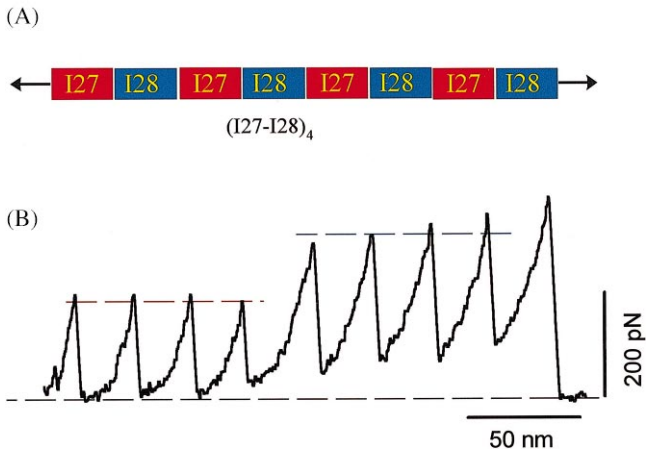

Fig. 3. The extension of a heterodimeric polyprotein rules out desorption as an explanation for the force spectroscopy observations. (A) Schematic diagram of the $(I27–I28)_4$ polyprotein. (B) The force–extension curve of a full length $(I27–I28)_4$ polyprotein shows two levels of unfolding forces (pulling speed: 0.6 nm/ms) with the less stable domains unfolding first (at about 200 pN, as expected for the I27 domain) followed by the more stable domains (at about 300 pN, close to that expected for I28). The unfolding of domains according to their mechanical stability, irrespective of their order in the heteropolyprotein, is inconsistent with an alternative hypothesis in which the force peaks represent detachment of modules adsorbed to the substrate. Note that the last peak corresponds to the extension and detachment of the fully unfolded protein from the AFM tip.

folds, as we will show in this review. Whereas I27 domains unfold at ~200 pN with spacing of 28.1 nm, the corresponding values for the C2A domain are ~60 pN and 38 nm and <20 pN and unknown for calmodulin.

Taken together, these observations effectively rule out the possibility that the AFM observations are an artifact of desorption from the substrate.

3.3. Does the pulling geometry affect the AFM measurements?

In our discussion up to now we have assumed an orthogonal geometry of pulling, i.e. that the polyprotein is being pulled at a 90° angle, with the two attachment points of the protein (to the cantilever tip and to the substrate) in a vertical line. A more realistic picture is that the polyprotein would be pulled at a slight angle. Fig. 4A illustrates this point. Prior to extension, the distance between the two ends of a folded domain will be 4.4 nm (as estimated by NMR; Improta et al., 1996). The angle between the fully extended domain (28.1 nm) and the substrate will therefore be 77° (see Fig. 4B). This angle would result in an error in the estimate of protein length of less than 1%, which represents the worst-case scenario. In a multidomain protein the maximum distance between the attachment points will be given by 4.4 nm multiplied by the number of modules; the proportional increase and therefore the angle of extension would remain the same. Such geometrical errors in the alignment of the attachment points are therefore negligible for our measurements.

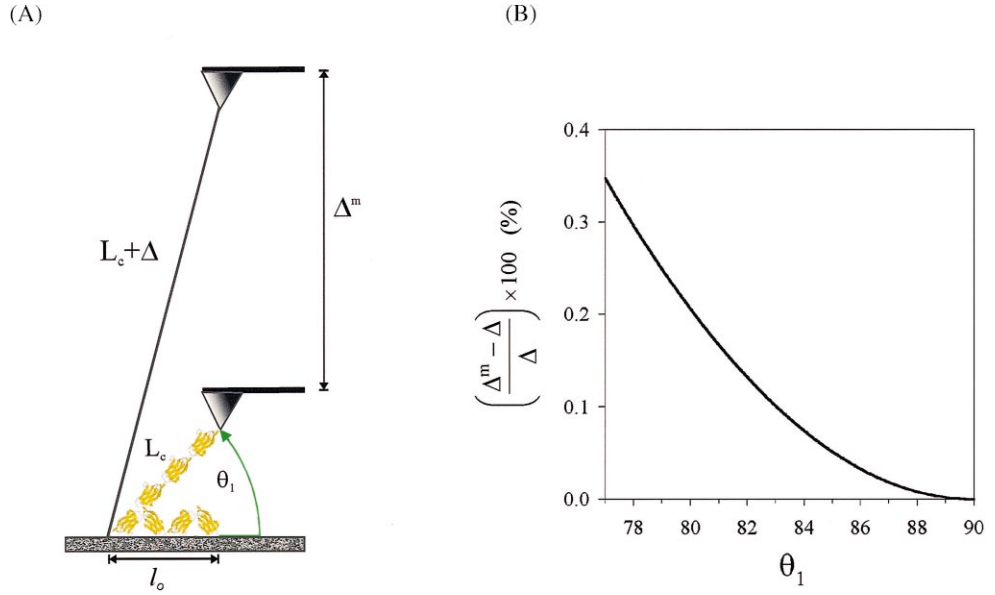

Fig. 4. Geometrical errors in the measurements of the contour length of a polyprotein. (A) A relaxed polyprotein with a length l_0 is picked up by the AFM tip and stretched by force to a folded contour length L_c. The stretched polyprotein is pulled at an angle θ_1. Module unfolding extends the protein to a contour length $L_c+\Delta$. The measured increase, Δ^m, is a function of θ_1. (B) We calculate this error as a function of θ_1 for a typical polyprotein composed of 10 identical I27 domains with a random end-to-end length of $l_0 = 8.6$ nm and a contour length of $L_c = 38$ nm and $\Delta = 280$ nm. Under these conditions, the maximal error in the measurement of Δ occurs at a $\theta_1 = 77^\circ$ and is less than 1%. Molecules stretched at higher θ_1 values have a lower error. When $\theta_1 = 90^\circ$ the theoretical error is zero (see text). Modified from Carrion-Vazquez et al. (1999b).

4. Constructing polyproteins

Most of the reported methods to synthesize tandem repeats of a DNA sequence are laborious and have therefore been used only rarely (Graham and Maio, 1992). The method we use routinely is based in a single-step cloning of Ava I concatemers (Hartley and Gregori, 1981) into a custom-made expression vector (Carrion-Vazquez et al., 1999a).

Our method relies on the concatemerization of DNA monomers, flanked by restriction enzyme sticky ends, using in vitro self-ligation. The restriction enzyme Ava I is used since its restriction site is asymmetrical, allowing directional assembly of the monomers (i.e., head to tail). Monomers of the expressed polyprotein will therefore be connected by a Leu-Gly linker, which corresponds to the translation of codons of the Ava I site. This technique was originally reported by Hartley and Gregori (1981) and considered as one of the most reliable methods to make tandem repeats of a DNA sequence (Graham and Maio, 1992). Fig. 5A shows a ladder of ligation products separated by analytical electrophoresis on an agarose gel.

pET vectors are considered to be the most powerful system developed for cloning and expression of recombinant proteins in *E. coli* (Studier et al., 1990). A new pET vector tailored to our specific needs was constructed (“pET Ava I”). This consists of a short His-tag on the N-terminus (for the affinity purification of the protein), an enterokinase site (for the eventual cleavage

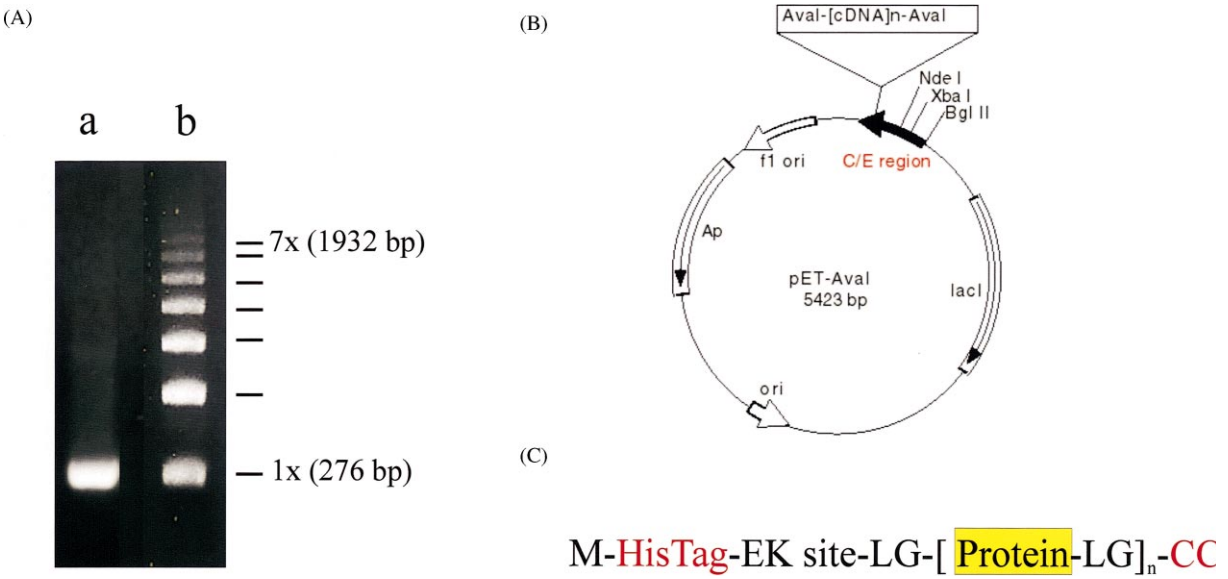

Fig. 5. Engineering polyproteins for AFM. (A) Directional DNA concatemerization of monomers is done by self-ligation of the sticky ends of the nonpalindromic CTCGGG *Ava*I restriction site. This figure shows an agarose gel stained with ethidium bromide showing the I27 monomer (lane a) and a ladder of concatemers with various numbers of I27 monomers (lane b). (B) Map of our custom-made expression vector designed for single-step cloning of the Ava I concatemers. Its cloning/expression region includes an N-terminal His-tag (for affinity purification of the polyprotein), an enterokinase site (for easy cleavage of the His-tag out of the fusion protein), the CTCGGG AvaI cloning site, two cysteine residues at the C-terminus (for covalent attachment of the polyprotein to gold-coated coverslips) and a stop codon. (C) Structure of the repetitive protein generated by this method.

of the His-tag), a unique CTCGGG Ava I cloning site (for cloning of the Ava I multimers), and two cysteine residues on the C-terminus (for the covalent attachment of the polyprotein to gold coated coverslips) (Fig. 5B). The resulting polyproteins have a short His-tag and an enterokinase site on the N-terminus, two cysteine residues on the C-terminus, and a Leu-Gly linker between monomers (Fig. 5C). There is evidence that such His-tags remain unstructured in solution and do not affect the properties of the flanking regions (Politou et al., 1994a,b, 1996; Improta et al., 1996).

The first step in this method is the synthesis by PCR of the monomer carrying CTCGGG Ava I sites on both ends. After Ava I digestion, the sticky-ended monomer is gel purified and then self-ligated at high concentration. These concatemers are then ligated into "pET Ava I" and then transformed into a recombinase-defective *E. coli* cloning strain to prevent the deletion of tandem repeats by recombination. Clones bearing high-order multimers are selected and transformed into a recombinase-defective expression strain to express the polyprotein. Purification is usually done specifically by affinity chromatography using Ni^{2+}-columns, which bind the His-tagged polyproteins.

4.1. Construction of Ava I monomers

The first step in our method is the synthesis of PCR mutagenic primers bearing the appropriate sequence modifications to include the Ava I nonpalindromic sites at both ends. Since the fidelity

of copy is critical in protein expression, we use for this amplification Pfu DNA polymerase (Stratagene), which has the lowest error rate available due to its proofreading activity. We have used three different PCR templates in our studies: titin template was a cDNA insert carrying 8 Ig domains (I27–I34) of human cardiac titin in a pET plasmid [I27–I34-CC/pET8c-(His)], obtained from Dr. M. Gautel (Rief et al., 1997a). The calmodulin template was a cDNA encoding rat calmodulin in a pET 14b plasmid (pETCM clone), obtained from Dr. K. Titani (Hayashi et al., 1998). The C2A template was a cDNA clone from rat synaptotagmin I (pCMV65-5 clone), obtained from Dr. T.H. Südhof (Perin et al., 1990). For I27 and calmodulin an extra Gly codon was added upstream of the Leu-Gly linker encoded by the Ava I site.

The PCR products were subcloned and sequenced following standard techniques (Sambrook et al., 1989).

4.2. Synthesis of concatemers

The subcloned monomers are digested with Ava I, gel purified and self-ligated overnight at 16°C. Ligation products are then separated by analytical electrophoresis in an agarose gel and stained with ethidium bromide.

To prevent self-ligation of the concatemers, which would result in circular concatemers unable to ligate into a vector, we start with a high concentration of monomers.

4.3. Cloning of concatemers into pET Ava I

The Ava I concatemers are subcloned into a dephosphorylated pET Ava I expression vector (Fig. 5B) by bulk ligation. The ligation products are transformed into SURE 2 (rec B^-, rec J^-) supercompetent cells (Stratagene) and the colonies analyzed directly by DNA purification and restriction digestion or by PCR colony screening using Platinum Taq DNA polymerase (Gibco-BRL). This is the most critical and tedious step since bulk ligation is used. We typically screen 50–300 clones to get a concatemer of eight or more monomers.

4.4. Expression and purification of polyproteins

Clones carrying the appropriate multimeric insert are transformed into BLR(DE3) competent cells (rec A^-) for expression. Expression is then induced in an exponential culture in the presence of 1 mM IPTG. Cells are lysed by sonication and the lysate is centrifuged to collect the soluble fraction, which frequently contains most of the recombinant protein. Polyproteins are then purified from this fraction using Ni^{2+}-affinity chromatography (Novagene). Calmodulin was also purified by phenyl-sepharose hydrophobic chromatography (Pharmacia) according to Gopalakrishna and Anderson (1982). Proteins were analyzed by SDS-PAGE, concentrated and dialyzed into the final buffer by ultrafiltration using Centriplus and Microcon (Amicon-Millipore). The final buffer was either PBS/5 mM DTT or 0.1 M imidazole pH 6.0 for poly-I27 and poly-C2A, and 0.1 M Tris pH 7.5 for calmodulin.

5. Protein folds have different mechanical stability

In this section we will discuss the mechanical properties of three different folds. Two of them are considered to be "all beta" structures (Murzin et al., 1995; Bateman et al., 1999) and have a so-called β-sandwich topology. One of them is from a typical mechanical protein (an immunoglobulin domain from titin) and the other from a protein involved in secretion (the C2A domain from synaptotagmin I). The third case is calmodulin, a ubiquitous regulatory protein considered to be an "all alpha" protein.

5.1. Titin immunoglobulin domains present high mechanical stability

The immunoglobulin (Ig) domain is one of the most abundant protein modules in nature, being present in a large variety of proteins including antibodies, cell adhesion molecules, cell surface receptors, enzymes, chaperones and muscle proteins (Bork et al., 1994: Gerstein and Levitt, 1997). The Ig superfamily consists of several topologies; the "I" set ("intermediate") is considered to have the ancestral topology, based on its hybrid structure (i.e., it combines features from all the other topological classes) and on phylogenetic comparisons (Chothia and Jones, 1997). The I set, which includes the majority of Ig domains occurring in cell adhesion proteins, surface receptors and muscle proteins (Harpaz and Chothia, 1994), was the first topology to be analyzed in detail by AFM in the muscle protein titin (Rief et al., 1997a).

Titin is a gigantic modular protein ($\sim$3000 kDa) responsible for the passive elastic properties of muscle (reviewed in Trinick and Tskhovrebova, 1999). Although the molecular determinants of titin elasticity are still a matter of debate (reviewed in Horowits, 1999; Trinick and Tskhovrebova, 1999; Linke, 2000), recent results show that unfolding of just a few Ig modules could fully account for the viscoelastic properties of skeletal myofibers (Minajeva et al., submitted). Furthermore, there is some evidence that the unfolding/refolding of Ig modules could occur in the physiological range of force (Linke et al., 1996). AFM studies have shown that a group of I-type Ig modules from human cardiac titin (I27–I34; "I" refers here to the sarcomeric I band, not to the aforementioned "intermediate" topology) displays a hierarchical ordering of mechanical stability from low (150 pN) to high (300 pN) unfolding forces (Rief et al., 1997a). AFM could not, however, establish the correspondence between force peaks and modules to identify the individual stability of specific modules. As we have already discussed, the solution to this problem came from molecular biology.

5.1.1. The I27 module

The I27 module of human cardiac titin was originally chosen for AFM studies because it is very stable thermodynamically (melting point, 73°C; Politou et al., 1995), its tertiary structure had been already established by NMR spectroscopy (Improta et al., 1996), and its stretching had been simulated using a technique known as steered molecular dynamics (SMD; Lu et al., 1998).

The I27 module, which is 89 amino acids long, has a typical Ig I topology composed of seven β-strands (strands A–G), which fold into two face-to-face β-sheets through backbone hydrogen bonds and hydrophobic core interactions (Fig. 6C). With the exception of the parallel pair A′G, all adjacent β-strands in both sheets are antiparallel ("parallel" and "antiparallel" refer to the orientations of two apposed strands with respect to their N- and C-termini; two strands that are

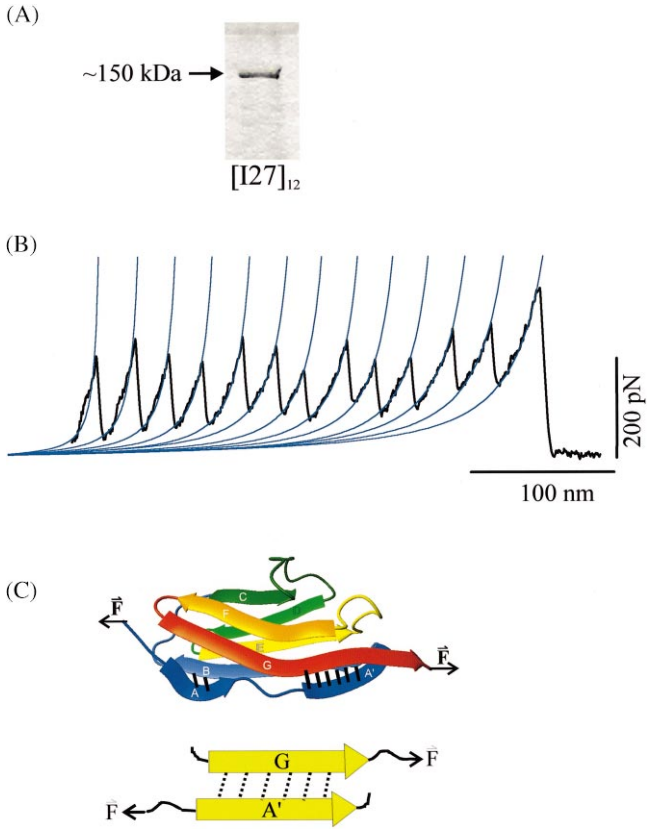

Fig. 6. Mechanical properties of single human cardiac titin immunoglobulin domains. (A) Coomassie blue staining of the purified $I27_{12}$ protein separated using SDS-PAGE. The measured molecular weight of the polyprotein (~150,000) is in good agreement with the predicted molecular weight of a $I27_{12}$ concatemer including a His-tag-EK region, 13 GLG linkers, and 2 terminal cysteine residues. (B) Stretching $I27_{12}$ with AFM (at a pulling speed of 0.6 nm/m s) resulted in a force-extension curve with peaks that vary randomly in amplitude about a value of 204 ± 26 pN ($n = 266$). The last peak represents the final extension of the unfolded protein prior to detachment from the AFM tip. Note the random distribution of the unfolding forces for each peak and the deviation from entropic behaviour (''the hump'') evident in the early peaks. Fits of the WLC model to the force-extension curves of $I27_{12}$ give a persistence length of $p = 0.39 \pm 0.07$ nm ($n = 10$) and a variable contour length of $L_c = 25$ to 496 nm (blue lines). Consecutive peaks were fitted by the WLC with the same persistence length and a contour length increment of $\Delta L_c = 28.1 \pm 0.17$ nm ($n = 16$). The persistence length is a measure of the distance over which the polymer retains memory of a direction. This persistence length is of the size of a single amino acid (0.40 nm). (C) The mechanical topology of I27. Top. 3-D structure of titin I27 domain (from SCOP database; Murzin et al., 1995) showing the ''shear pattern'' model for the H-bond breakage in the I27 domain, where the H-bonds break simultaneously. Seven β-strands (each of them shown as a ribbon arrow of a different color) are folded into two β-sheets, one comprising strands A,B,D,E and the other including strands A′,C,F,G. The dashed lines depict the topology of the critical H-bonds between β-strands under an applied force. Bottom. Detail of the hydrogen bond patch between A′ and G strands are shown as discontinuous lines. The direction and sense of the applied force is indicated by black arrows.

oriented in the same direction are parallel while strands oriented in opposite direction are antiparallel). SMD simulations identified the interactions likely to underlie the mechanical stability of I27 (Lu et al., 1998). Simulations of the application of axial force to the terminal ends of this module showed that a critical set of six hydrogen bonds, linking strands A′ and G, provided the point of maximal resistance to unfolding. Since the hydrogen bonds in this patch are perpendicular to the direction of the applied force (a "shear" topology), unfolding requires the simultaneous rupture of this cluster of hydrogen bonds (see Fig. 6C, bottom). Upon the rupture of this patch of hydrogen bonds, the rest of the folded polypeptide unravels with little resistance. These theoretical predictions fit well with experimental observations (Carrion-Vazquez et al., 1999a,b) as is described below. A similar hydrogen-bonding topology has been proposed, based on X-ray crystallography, for the first Ig domain of the adhesion protein ICAM-1 (Casasnovas et al., 1998).

5.1.1.1. Polyproteins demonstrate the stochastic nature of mechanical unfolding. To analyze the mechanical properties of the I27 domain by AFM, we constructed a $I27_{12}$ polyprotein, as discussed in Section 4 (Fig. 6A). In this construct, an additional glycine residue was added to the linker (GLG instead of LG) to more closely mimic the GGG linkers used in previous studies (Improta et al., 1998). Electron micrographs of rotary shadowed $I27_{12}$ show rod-like structures $\sim$58 nm in length (H. Erickson, pers. comm.), which corresponds well to the expected length based on the NMR spectroscopic measurements of single I27 modules (each of which has a length of 4.4 nm; Improta et al., 1998).

Random segments of the $I27_{12}$ polyprotein were picked up by adsorption to the AFM tip. The resulting force–extension curves showed a saw-tooth pattern with as many as 12 equally spaced force peaks. The fitting of consecutive unfolding peaks to the WLC model showed that each unfolding event added 28.1 ± 0.17 nm to the protein length. The unfolding force varied randomly around a mean value of $\sim$200 pN (Fig. 6B). A histogram of force peaks (unfolding force) revealed an asymmetrical distribution of events with a maximum at about $\sim$200 pN (Carrion-Vazquez et al., 1999a), which is in contrast to the pattern of rising forces observed with the I27–I34 titin recombinant fragment, where peaks ranged from 150 pN to 300 pN (Rief et al., 1997a). These experiments demonstrate that domain unfolding does not occur above a "threshold force" but rather is a probabilistic event, which may therefore be observed at any force, albeit with different probability (Carrion-Vazquez et al., 1999a). The force at which an unfolding event occurs reflects the mechanical stability of a particular folded module under the specific experimental conditions used. The unfolding force, and therefore the mechanical stability, depends on the rate of extension, the faster the pulling speed, the higher the force required to cause the unfolding of the domain.

5.1.1.2. Polyproteins spontaneously refold upon relaxation. The domains of modular proteins like titin have been proposed to undergo many unfolding/refolding cycles during their physiological activity (Erickson, 1994). The refolding process can be reproduced in vitro by AFM in both native modular proteins (Rief et al., 1997a; Oberhauser et al., 1998) and polyproteins (Carrion-Vazquez et al., 1999a). Once the polyprotein has been stretched and its domains unraveled, it can be relaxed by returning the substrate to the original position. The unfolded domains recover their

fold spontaneously in a time-dependent fashion with the proportion of recovered modules depending on the relaxation time between extensions. This procedure can be repeated several times, allowing the measurement of the refolding rate of individual protein domains.

5.1.1.3. Is the fidelity of refolding decreased in polyproteins?. Since native modular proteins are not strictly repetitive, it could be argued that the repetitive nature of polyproteins could favor abnormal intermodule refolding. AFM refolding experiments with poly-I27 have identified missing peaks (''skips'') in their force–extension curves (Oberhauser et al., 1999). The interval between peaks in a skip corresponds to the size of two I27 domains plus the length of the linker between domains. This suggests that skips represent misfolding events in which the A′ strand of one domain binds with the G strand of the adjacent domain creating a larger fold with a stability similar to that of the native I27. However, the frequency of skips in poly-I27 (~2%) was found to be of the same order as that of the FN-III domains of tenascin (~4%) indicating that the frequency of misfolding is not higher in polyproteins than in heterogeneous modular proteins.

5.1.1.4. Polyproteins allow an accurate analysis of the unfolding kinetics. The unfolding of a domain under an applied force is a probabilistic event that can be modeled as a two-state process with a rate that depends exponentially on the axial force and the unfolding distance along which the force is applied. This description gives a probability of observing an unfolding event as $P = N\alpha\Delta t$, where N is the number of modules, Δt the pulling interval, and α is the unfolding rate constant. The unfolding rate constant at a given force is given by $\alpha(F) = \alpha_0 e^{F\Delta x/kT}$. For a given α_0 (unfolding rate at zero force), if the unfolding distance (Δx, the extension required to disrupt the fold) is small, the force of unfolding will be high, while if the forces that maintain the fold are distributed over a greater distance the unfolding force will be lower.

One can model the probability of unfolding versus the applied force using Monte Carlo techniques to estimate the unfolding distance and the unfolding rate at zero force (Rief et al., 1997; Oberhauser et al., 1998; Kellermayer et al., 1997). The best fit for the histogram of unfolding forces for I27 was obtained using an unfolding rate at zero force of $3.3 \times 10^{-4}\,s^{-1}$ and an unfolding distance of 0.25 nm (Carrion-Vazquez et al., 1999a).

The short unfolding distance measured for I27 (roughly the size of a molecule of H_2O) is consistent with the SMD simulations (Lu et al., 1998), which predict that unfolding occurs as a single event with low force after the rupture of the hydrogen bonds of the A′G patch. Furthermore, the interval between peaks (28.1 ± 0.17 nm) observed using AFM suggests an elongation of 70 amino acids, considering that the length of an amino acid residue is 0.40 nm (see Section 5.1.1.5.) ($70 \times 0.40\,nm \approx 28.1\,nm$). This agrees well with the length of the ''force hidden'' region predicted by the SMD simulation (about 72 amino acids; there is uncertainty in the boundaries of this region).

5.1.1.5. Amplification by polyproteins allows the mechanical dissection of a fold with amino acid resolution. To demonstrate the validity of this structural model, and to measure the spatial resolution of the AFM, a mutant polyprotein was constructed in which a cluster of 5 glycine residues was inserted into the hairpin loop joining the F and G β-strands of I27, which is within the predicted ''force-hidden'' region. The interval between force peaks was lengthened, on average, by 2.00 nm per domain. This value can be used to estimate the length of an amino acid

residue (2.00 nm/5 = 0.40 nm). The length 0.40 ± 0.06 nm obtained this way is somewhat bigger than that determined from the geometry of the polypeptide chain (0.36 nm; Oesterhelt et al., 2000). The difference is potentially due to the stretching of amino acid residues by the external force, and partially it originates from applying the WLC model to determine the contour length of the protein. Since this caliper, 0.40 nm/amino acid residue, already includes all uncertainties of our methodology, it can be used confidently to count the number of amino acids.

The corresponding control polyproteins in which the glycine cluster was inserted before or after the A′G patch (i.e., outside the force-hidden fold) did not show an increase in the unfolding interval, presumably because these regions are already pre-stretched before unfolding takes place (Fig. 7; Carrion-Vazquez et al., 1999b).

These experiments reveal the remarkable resolution (i.e., to the amino acid level) attainable in AFM by using polyproteins to amplify linearly the mechanical features of a single module.

5.1.1.6. Amplification by polyproteins allows the study of unfolding intermediates. In addition to a major force barrier to unfolding, SMD simulations (Lu et al., 1998) predict that a weaker barrier, the AB patch, which consists of two H-bonds in a shear topology (see Fig. 6C), should be disrupted by force-induced extension prior to the rupture of the A′G patch. Linear amplification by polyproteins allowed this phenomenon to be observed and analyzed. The first unfolding peaks in Fig. 6B show clear deviations from the entropic behavior predicted by the WLC model of polymer elasticity. These "humps" of low force (~100 pN) are likely to represent simultaneous rupture of the AB hydrogen bonds in each of the domains. The presence of a smaller hump in subsequent unfolding events suggests that the remaining domains refold very quickly to their native conformation before the next unfolding event occurs. This hypothesis was confirmed by site-directed mutagenesis with the construction of a mutant polyprotein in which a proline substitution disrupting the AB patch abolished the hump (Marszalek et al., 1999b).

The molecular determinants of titin elasticity are poorly understood (Trinick and Tskhovrebova, 1999; Horowits, 1999). In cardiac titin, three regions have been proposed to be responsible for the global elastic properties of the molecule: the Ig domains and the so-called PEVK and N2B regions (Granzier et al., 1997; Linke et al., 1999). The discovery of this unfolding intermediate in Ig modules of titin uncovers a new elastic component in this protein that occurs at lower forces prior to unfolding and would result in an extension similar in size to that generated by the elongation of the PEVK region in cardiac titin (Marszalek et al., 1999b).

5.1.1.7. Hydrogen bonding pattern and the mechanical properties of I27. As discussed above, SMD simulations (Lu et al., 1998) predict that there are two patches of hydrogen bonds that are relevant for the mechanical properties of I27 (Fig. 6C, top). As the fold is stretched, the AB patch unfolds first, at low force (~100 pN), causing deformation of the first peaks (the "hump"). At higher forces (~200 pN) the A′G patch is disrupted and the hydrophobic core unfolds with little resistance. The topology of these hydrogen bond patches appears to be critical to understanding the mechanical properties of I27. The SMD studies predict that the simultaneous breakage of the A′G cluster of H-bonds causes the high-energy barrier opposing the forced unfolding of the I27 domain (Fig. 6C, bottom). This simultaneous H-bond rupture would require higher force than a sequential pattern of breakage, in which the H-bonds break one after the other (see below) (Lu and Schulten, 1999). The AB patch, which has only two H-bonds in a shear topology, unfolds

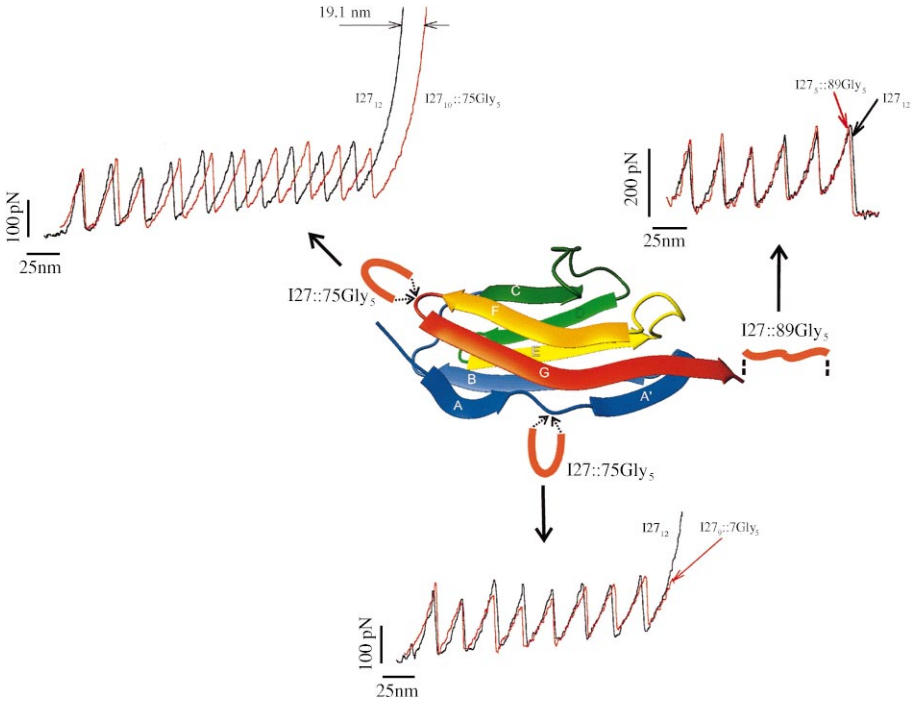

Fig. 7. Direct observation of a length phenotype in an immunoglobulin module. (Center) Structure of the I27 immunoglobulin module and location of the glycine insertion sites. The N- and the C-termini of I27 are parallel and are in close apposition over the A′G strands. A mechanical linkage between the A′ and G strands is thought to provide continuity of force between the N- and C-termini of the folded module. Rupture of this linkage exposes the amino acids that are hidden in the fold, extending the contour length of the protein. We constructed polyproteins based on the wild type (I27) and mutant forms of the I27 module with a Gly_5 insert in the FG hairpin loop at position 75 (I27::$75Gly_5$), in the N-terminal region at position 7 (I27::$7Gly_5$), and after the C-terminus at position 89 (I27::$89Gly_5$). (Top left) Insertion of 5 glycine residues into the FG loop of the I27 module increases the contour length of the unfolded module by ~2 nm (5×0.40 nm). A comparison of the force–extension curves of a wild type I27 polyprotein ($I27_{12}$; black trace) and a mutant polyprotein, $I27_{10}$::$75Gly_5$ (red trace), shows that the mutant polyprotein extends more with each unfolding event. After 10 consecutive unfolding events, this particular mutant polyprotein is 19.1 nm longer than the wild type polyprotein (arrows), corresponding to a difference of 1.91 nm/module. (Top right and bottom) The saw-tooth pattern in the force-extension curves obtained from polyproteins engineered with 5 glycine insertions placed either in position 89 ($I27_5$::$89Gly_5$; red trace in top right traces) or in position 7 ($I27_9$::$7Gly_5$; red trace in bottom traces) superimposed on the saw-tooth pattern obtained from the wild type polyprotein ($I27_{12}$; black trace).

with less force that the A′G patch, which has six H-bonds with the same mechanical topology (Fig. 6C).

Proline mutagenesis has been used to test the hypothesis that backbone hydrogen bonds are responsible for the two mechanical barriers present during the unfolding of the I27 module. As mentioned, a proline substitution in the A strand, to prevent the interaction with the B strand, abolished the formation of the low force barrier (Marszalek et al., 1999b). When valines at positions 11, 13 and 15 of the A′ strand were substituted by prolines, to prevent the formation of hydrogen bonds with the G strand, the force required to unfold the domain was decreased, as expected. However, a mutation of tyrosine to proline in position 9 actually increased the

mechanical stability of the domain (Li et al., in press). This result indicates that other non-covalent interactions may also contribute to the mechanical resistance of the fold.

5.1.2. Mechanical properties of other titin modules

Ig-like domains of the Ig and FN-III types are 7-stranded β-sandwich structures with the N- and C-terminal strands parallel to each other and pointing in opposite directions. These domains seem to have evolved to withstand forces when connected in series and, because of the shear topology of their critical hydrogen bonds, these domains offer a high resistance to mechanical stretching (Rief et al., 1997a, 1998; Oberhauser et al., 1998; Carrion-Vazquez et al., 1999a). Interestingly, Ig domains that occur in muscle proteins, cell adhesion proteins, and surface receptors usually belong to the "I" class (Harpaz and Chothia, 1994) and are likely to have a similar mechanical topology.

By engineering polyproteins it has been possible to analyze in detail the molecular determinants of the elastic properties of one of those modules, the I27. What can be expected from the study of the mechanical properties of other modules? First of all we need to consider that homologous titin modules from distant species (orthologs) are much more similar than analogous repeats within the same species (paralogs) (Witt et al., 1998). This observation indicates that the specific amino acid sequence of each of the titin modules has been subject to strong selective pressure through evolution and therefore may be relevant for function. Since the main function of titin seems to be mechanical, the primary structure of each of its modules may be critical for determining its mechanical properties. Hence each of titin Ig modules seems to contribute a specific mechanical stability to the passive elastic properties of titin and may not be merely equivalent repetitions. AFM experiments using polyproteins from a contiguous module, the I28, show that it unfolds at higher forces ($\sim$260 pN) and presents a more stable "hump" ($\sim$150 pN) (Marszalek et al., 1999b). Future structural information about I28 could shed light into the molecular origin of these differential properties. Further research will also be necessary in order to understand how these properties can be related to the global elastic properties of titin. The first clues towards the understanding of this combinatorial logic come from AFM experiments using a heterodimeric polyprotein I27–I28 (Fig. 3). The mechanical stability of the I28 in this chimera is increased to $\sim$300 pN. Therefore, it seems that the topological connectedness of modules is a critical factor for their mechanical stability (Li et al., 2000).

5.2. The mechanical stability of other protein folds

Do Ig-like domains respond to stretching in a quantitatively different fashion than do domains that are not normally exposed to mechanical strain? To further understand the principles of the mechanical design of proteins a comparison was made with proteins that do not have a known mechanical function. Using the polyprotein approach, we investigated the C2A domain from synaptotagmin I and calmodulin.

5.2.1. The C2 domain: a fold with low mechanical stability

The C2 domain is a conserved "all beta" module present in more than 40 different proteins, many of them involved in membrane interactions and signal transduction (e.g. synaptotagmins, rabphilins, protein kinase C isozymes, phospholipase A_2, perforins). The first C2 domain of

synaptotagmin I (C2A) is believed to be the calcium sensor that initiates membrane fusion during neurotransmitter release (Sudhof and Rizo, 1996; Shao et al., 1996). The 3D structure of C2A was found to be a β-sandwich composed of 127 amino acids arranged into eight antiparallel strands with the N- and C-terminal strands pointing in the same direction (Fig. 8C, left; Sutton et al., 1995). In contrast to the I27 domain, in which the A′G patch of H-bonds have a "shear" topology, those in the AG patch of the C2A domain are in a "zipper" configuration (i.e., parallel to the direction of the applied force; Fig. 8C, right). SMD simulations (Lu and Schulten, 1999) predicted very low forces of unfolding for this domain. In AFM experiments the force–extension curve of C2A polyproteins showed a saw-tooth pattern with force peaks of ~60 pN separated by ~38 nm (Fig. 8B). The measured size of the folded core of the domain agrees well with that

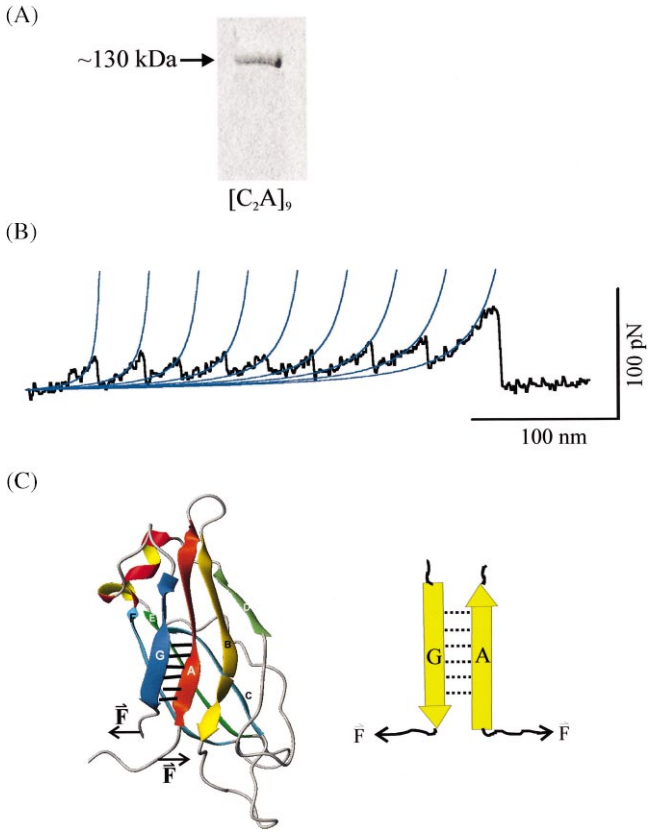

Fig. 8. Mechanical properties of a single I C2A domain. (A) Coomassie blue staining of the purified $C2A_9$ protein separated using SDS-PAGE. (B) Force–extension relationship for the C2A polyprotein measured with AFM (at a pulling speed of 0.6 nm/m). The saw-tooth pattern show peaks with an unfolding force of ~60 pN. Consecutive peaks were fitted by the WLC with the same persistence length ($p = 0.4$ nm) and a contour length increment of $\Delta L_c = 38$ nm. (C) Left. Schematic diagram of the topology of the β-sandwich structure of C2A domain (from SCOP database; Murzin et al., 1995). Right. The "zipper" model for the H-bond breakage in C2A domains in which each bond breaks sequentially. The hydrogen bonds between A and G strands are shown as black lines. The direction and sense of the applied force is indicated by the black arrows.

predicted based on the number of amino acids between the end of the A strand and the beginning of the G strand ($106 \times 0.4 = 42$ nm).

Circular permutants (e.g., topological mutant proteins that maintain the amino acid sequence with different N- and C-termini) of the C2A domain could be used to test the hypothesis of the lower mechanical resistance of the "β-zipper" versus the "β-shear" H-bonds in a β-barrel.

5.2.2. *Calmodulin: a compliant protein structure*

Calmodulin is a highly conserved antiparallel "all α" protein that acts as a primary calcium-dependent regulator of many intracellular processes. The three-dimensional structure of calmodulin (148 residues) is dumbbell shaped and consists of 7 α-helixes distributed in a helical central region capped by two globular regions, each containing two helix-loop-helix EF-hand motifs that are responsible for Ca^{2+}-binding (Fig. 9C, left; Babu et al., 1985, 1988). In contrast to the β-sandwich topology, where there is a nonhomogeneous distribution of the inter-strand H-bonds (in either shear or zipper configuration), the α-helix has a homogeneous distribution of intrahelix H-bonds. SMD simulations predict that stretching of the structure would cause sequential breaking of the intra-helix hydrogen bonds, leading to the elongation and separation of α-helices, a process that would require little force. The predicted unfolding pathway does not require breakage of clustered H-bonds (K. Schulten, personal communication) as was predicted by SMD for cytochrome c6, another all α-helical protein (Lu and Schulten, 1999). Therefore no force peaks are expected upon stretching of calmodulin.

To test these predictions a rat polycalmodulin (CaM_4) was constructed (Fig. 9A). CaM_4 was purified either by Ni^{2+}-affinity chromatography or by phenyl-shepharose affinity chromatography, with identical results. Only CaM bound to Ca^{2+} in its native conformation binds to phenyl-sepharose; CaM in the presence of low concentration of Ca^{2+} does not bind (Gopalakrishna and Anderson, 1982). The stretching of CaM_4 did not yield any force peaks, indicating that the unfolding forces must be below our AFM noise level ($\sim$20 pN). Only very compliant structures of the approximate size of the tetrameric polyprotein were found ($4 \times 148 \times 0.40 = 237$ nm) confirming SMD predictions (Fig. 9B). Both SMD and AFM therefore agree that calmodulin behaves like a random polypeptide chain under force. Unlike the I27 domain, whose tertiary fold has been designed to withstand force, calmodulin does not show mechanical barriers to prevent its unfolding. Paradoxically, one of the most striking characteristics of calmodulin is its thermodynamic stability, particularly in the presence of Ca^{2+}. The protein may be exposed to 95°C or to a 9 M urea solution with retention of biological activity (Wallace et al., 1980). The Ca^{2+}-free form of CaM has a melting temperature of $\sim$55°C, while the Ca^{2+}-bound form denatures only at temperatures exceeding 90°C (Brzeska et al., 1983). We have not detected, however, any difference in mechanical stability in the presence or absence of Ca^{2+}.

The only other α-helical structure that has been stretched by AFM is spectrin, a cytoskeletal protein. However, this protein forms bundles of α-helices, rather than single α-helices. The force–extension relationship of this protein showed very low force peaks (25–35 pN; Rief et al., 1999; Fisher et al., 1999b). This range of forces is intermediate between the compliance of a single α-helix and the low force range of a zipper β-sandwich.

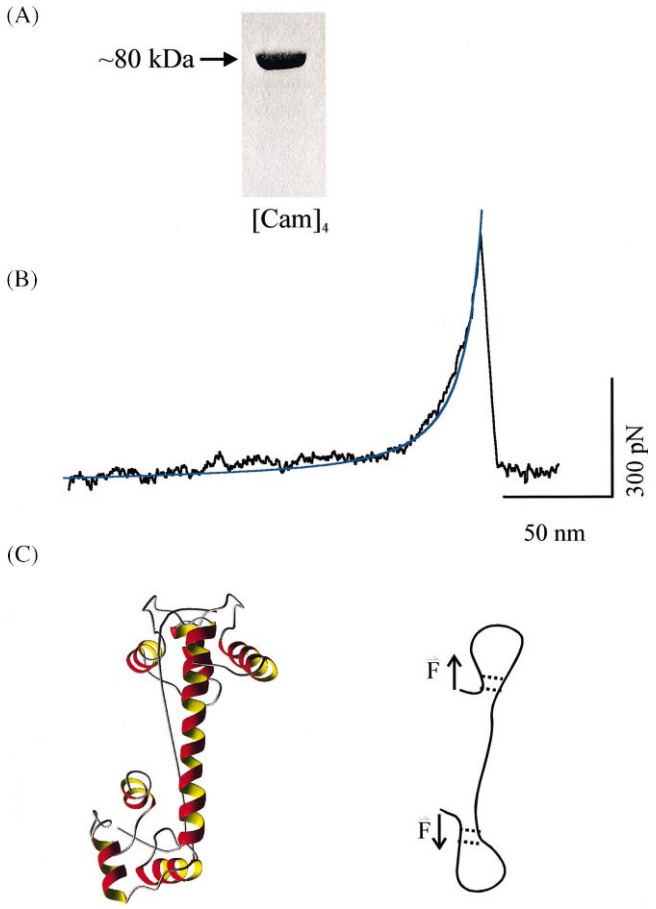

Fig. 9. The force-extension relationship for poly-calmodulin. (A) Coomassie blue staining of the purified CaM_4 protein separated using SDS-PAGE. (B) Stretching single calmodulin polyproteins (at a pulling speed of 0.6 nm/m s) give force–extension curves with no evident force-peaks. The force curve is well described by the WLC model (continuous lines) using a contour length of 212 nm (194 ± 15 nm, $n = 26$) and a persistence length of 0.32 nm. This contour length is similar to the expected contour length of a protein 580 amino acids in length (each CaM domain is 148 aa; 148aa $\times$ 4 monomers $\times$ 0.40 nm/residue = 237 nm). (C) Left. 3-D Structure of rat CaM showing its α-helical structure (from SCOP database; Murzin et al., 1995). CaM is made of seven antiparallel α-strands and two short antiparallel β-sheet hairpins with a ''zipper'' topology (not shown) that provide a structural link between the two Ca^{2+}- motifs (EF hands) of each globular region. Right. Putative mechanical topology of a calmodulin domain. The two small β-hairpins of calmodulin (see Fig. 8C, right) are in a ''zipper' configuration, and therefore should offer little resistance to mechanical unfolding.

6. The topological determinants of mechanical stability of proteins

Proteins are designed to perform specific biological functions and typically maintain a stable native conformation. In contrast, mechanical modules like the I27 of titin may be designed to undergo continuous unfolding/refolding cycles (Erickson, 1994). The topological design of this module includes two patches of H-bonds that act as mechanical barriers. One of these barriers, the AB patch, offers low resistance (~100 pN), while the A′G patch has a higher mechanical resistance

(~200 pN), which seems to protect the hydrophobic core from unfolding. It appears that proteins that experience mechanical stress (e.g., titin or ECM proteins) are composed of modules, like the I27 or FN-III, that are designed to withstand force while working in continuous unfolding/refolding cycles. They have strong backbone H-bonds patches that act as mechanical barriers to unfolding, with the β-shear H-bond topology being a stronger mechanical constraint than the zipper topology. An extreme case of a mechanical barrier to unfolding would be the disulphide bond, a covalent bond present in most Ig domains and other modules from antibodies, ECM and other extracellular proteins. The disulphide bond seems to have evolved to prevent the unfolding of the hydrophobic core over the physiological range of forces. Although the physiological role of a disulphide bond in a module is not clear, it may protect the mechanically isolated region (e.g., the hydrophobic core) from unfolding when the function of the protected region (e.g., ligand binding, dimerization) is incompatible with its mechanical unfolding.

In contrast, the proteins with no mechanical function that we have studied have very weak mechanical barriers to unfolding, as in the case of calmodulin. Between these two extremes there seems to be a spectrum of intermediate topologies, from the low resistance of the α-helical bundles of spectrin (25–35 pN) to the intermediate β-zippered sandwiches of the C2 domain (60 pN). Recently, an "alpha and beta" protein (Murzin et al., 1995), the bacteriophage T4 lysozyme, has been reported to exhibit unfolding forces of ~60 pN (Yang et al., 2000). Interestingly, this value is intermediate between the stability of the C2 domain and that of calmodulin, considering that the pulling speed in these experiments was about twice that used in our experiments (for a discussion on the dependence of the force with the pulling speed see Carrion-Vazquez et al., 1999a).

What are the physicochemical parameters that could help us to predict the mechanical stability of a module? The stability of a module, measured by equilibrium denaturation, may not be related to its probability of unfolding at a given force. We have found that mechanical stability does not necessarily correlate with thermodynamic stability. For example, the kinetic stability (during mechanical unfolding) of I27 and I28 is about 22.2 and 23.7 kcal/mol (Li et al., 2000), while their thermodynamic stability is about 7.6 and 3.0 kcal/mol, respectively (the melting temperatures of these modules are 72.6 and 54.1°C, respectively; Politou et al., 1995, 1996). A lack of correlation between thermal and mechanical stability is also observed for the C2 domain, CaM (Table 1) and spectrin repeats, which present a melting temperature rather similar to that of I28 (53°C; DeSilva et al., 1997). Thermodynamic and kinetic stability does not always correlate (Jackson, 1998; Plaxco et al., 1998). For example, the 10th FN-III domain from fibronectin is 4 kcal/mol more stable than the third FN-III domain from tenascin, yet it unfolds two times faster (Clarke et al., 1999). Folding kinetic experiments provide detailed information that allows a reconstruction of the energy diagram for unfolding. In the case of I27 (and I28) both the height of the unfolding energy barrier and the position of the transition state are similar for chemical and mechanical unfolding (Carrion-Vazquez et al., 1999a; Li et al., 2000), which indicates that kinetic stability (i.e., the height of the unfolding energy barrier) may be a good predictor of mechanical stability. However, the chemical unfolding experiments can only define a "solvent exposure" reaction coordinate whereas AFM experiments define the reaction coordinate as length of the protein during extension (Carrion-Vazquez et al., 1999a).

SMD simulations predict very well the qualitative behavior of a protein domain under force but they predict unfolding forces that are ten times larger than those observed by AFM

Table 1
Mechanical stability of single domains and proteins compared with their thermodynamic stability[a]

Domain	Conformational topology	Mechanical topology	Melting Temp. T_m (°C)	Thermodynamic stability $\Delta G^{(H_2O)}$ (kcal/mol)	Unfolding force at 0.6 nm/m s (pN)	Kinetic stability $\Delta G^{F=0}$ (kcal/mol)
CaM	α-Helix	Zipper	55°C[b]		<20[c]	ND
			>90°C (+Ca^{2+})[b]	—		
C2A	β-Sandwich	Zipper	55°C[d]		~60[c]	ND
			74°C (+Ca^{2+})[d]	—		
127	β-Sandwich	Shear	72.6°C[e]	~7.6[e,f]	~200[g]	~22.2[g]
128	β-Sandwich	Shear	54.1°C[e]	~3.0[e,f]	~260[h,f]	~23.7[f]

[a] Major discrepancies are highlighted in bold. Note that thermal and chemical stability is not a good predictor of mechanical stability, which can be defined, as a first approximation, by the force necessary to unfold a domain (this unfolding force depends on the pulling speed).
[b] Data compiled from Brzeska et al. (1983).
[c] Data compiled from this study.
[d] Data compiled from Shao et al. (1996).
[e] Data compiled from Politou et al. (1995)
[f] Data compiled from Li et al. (2000).
[g] Data compiled from Carrion-Vazquez et al. (1999a).
[h] Data compiled from Marszalek et al. (1999).

(Lu et al., 1998). SMD simulations cover only a very brief length of time (~1 ns) and therefore cannot fully incorporate contributions of the thermal motion (entropy) to the unfolding event. Furthermore, due to the brief simulation times involved, SMD cannot simulate the folding reaction.

We are just starting to understand the characteristics that define an elastic domain. For a given mechanical stability, the force of unfolding will be high if the disruption of the fold requires little extension, and will be lower if the forces that maintain the fold are distributed over a longer unfolding distance. The force required to unfold a domain is therefore highly dependent on the topology of the H-bonds within the fold. The spatial orientation (relative to the force vector), number, location and strength of these bonds appears to determine not only the mechanical stability, but also the dependence of the rates of unfolding and refolding on the applied force.

7. Conclusions

Force spectroscopy has been used to study the mechanical properties of heterogeneous populations of modules in modular proteins with known mechanical roles. The construction of homomeric polyproteins, using recombinant DNA technology, has recently allowed the study of the mechanical properties of a single module of the muscle protein titin (i.e., I27). We have applied this technology to proteins and domains with no known mechanical function, the C2A domain of synaptotagmin I and calmodulin. In contrast to the mechanical stability of I27, which requires forces of about 200 pN for unfolding, the C2 domain was found to be less stable (~60 pN) while calmodulin was mechanically compliant, with no force peaks present (<20 pN), at similar extension rates (0.6 nm/ms). These results indicate that the interactions that resist mechanical unfolding in an α-helix (calmodulin) are much weaker than those maintaining the structure of a zipper H-bonded β-sandwich (C2A domain), which is in turn less stable than a shear H-bonded β-sandwich topology (I27). We also have compared the mechanical stability of these structures with their thermodynamic and kinetic stability and conclude that the mechanical stability of a protein fold is not directly correlated with its thermodynamic stability but with its kinetic stability, which seems to be determined by its topology, the spatial pattern of its backbone hydrogen-bonding.

7.1. A niche for single-molecule force spectroscopy in the analysis of protein structure and dynamics

As an analytical tool, the primary attribute of AFM is that it provides mechanical information from individual molecules, not vast ensembles. This is the case for structural techniques, whether the molecules are ordered as in X-ray crystallography or dispersed as in NMR spectroscopy, and for techniques for monitoring protein folding, such as stopped-flow fluorimetry. AFM provides both structural (mechanical topology) and functional (mechanical properties) information from single protein domains in aqueous solution and in real time. Therefore, AFM promises, in theory, the possibility of directly probing the so-called folding energy landscape (Brockwell et al., 2000).

In spite of its recent progress, force spectroscopy is a developing technique still in its infancy. There is ample room for technical improvements in both the AFM setup (instrumentation,

recording techniques, analysis software, etc.) and in protein engineering (polyprotein construction, conditions to favor native folding, protein attachment and orientation, etc.). An ongoing development with future potential is the combination of force spectroscopy with fluorescence dynamics at the single-molecule level (Brockwell et al., 2000).

7.2. Perspectives

Current research in molecular biology is highly engaged in compiling a "horizontal", rather descriptive, catalog of protein sequences with their biological roles, but the "vertical" investigation of the physicochemical mechanisms of how proteins perform their functions (i.e., what eventually would allow us to understand biological systems at a deeper level) is in danger of falling behind. In particular, we expect that the analysis of the mechanical properties of protein folds will uncover in the near future a variety of architectures and structural elements and will set the foundations for a "mechanical biochemistry" of proteins. We are likely to encounter a variety of mechanical topologies in proteins inside and outside the cell to prevent unwanted unfolding, or to provide elasticity.

Mechanical unfolding in modular proteins has been proposed to modulate the kinetics of the interactions with their receptors or ligands (Oberhauser et al., 1998). Thus, mechanical design may be crucial not only for known mechanical proteins but for the regulation of the lifetime of protein-ligand interactions and for the function of the tensed network that, via cell-adhesion receptors and ECM proteins, supports mechanochemical sensing and transduction (Chicurel et al., 1998). Mechanical unfolding of protein modules may also be responsible for the high tensile strength and high toughness of natural adhesives (Smith et al., 1999). Research in these areas promises a broad spectrum of applications ranging from industry (e.g., development of glues with new properties) to medicine (e.g., high-resistance organic materials for orthopedics or dentistry).

Furthermore, mechanical unfolding in the cell may not be limited to proteins with a mechanical function. Most proteins in the cell seem to be mechanically unfolded at some point or another during their lifespan. Several cell compartments (i.e., endoplasmic reticulum, mitocondrion, chloroplast and proteasome) possess protein translocases that appear to use mechanical forces to unfold proteins during their normal turnover, typically prior to their assisted folding by chaperones or to their degradation (Rothman and Kornberg, 1986; Glick, 1995; Pfanner and Meijer, 1995; Baumeister et al., 1997; Shtilerman et al., 1999). The "nanomachinery" involved in this process is still poorly understood and, although the pulling geometry in vivo may be different, progress in force spectroscopy may benefit also our understanding of these biological unfoldases and vice versa.

The mechanical design behind the structure of proteins with a mechanical function probably represents precise evolutionary solutions to a variety of mechanical challenges that organisms have encountered through their evolution. The combination of force spectroscopy and molecular biology has now opened the way to the study of the mechanical properties of individual protein folds at the level of single molecules with nanoscopic resolution.

Acknowledgements

We are grateful to Drs. Mathias Gautel, Thomas H. Südhof and Koiti Titani for their generous gifts of the cDNA clones referred to in the text, and to Carmenlu Badilla-Fernandez and

William J. Greenleaf for excellent technical assistance. This work was funded by R01 grants from the National Institutes of Health to JMF, AFO and PEM, and by a National Science Foundation grant to PEM, JMF and AFO.

References

Babu, Y.S., Sack, J.S., Greenhough, T.J., Bugg, C.E., Means, A.R., Cook, W.J., 1985. Three-dimensional structure of calmodulin. Nature 315, 37–40.

Babu, Y.S., T.J., Bugg, C.E., Cook, W. J., 1988. Structure of calmodulin refined at 2.2 Å resolution. J. Mol. Biol. 204, 191–204.

Baljon, A.R.C., Robbins, M.O., 1996. Energy disipation during rupture of adhesive bonds. Science 271, 482–484.

Bateman, A., Birney, E., Durbin, R., Eddy, S.R., Finn, R.D., Sonnhammer, E.L., 1999. Pfam 3.1: 1313 multiple alignments match the majority of proteins. Nucleic Acid Res. 27, 260–262.

Baumeister, W., Cejka, Z., Kania, M., Seemüller, E., 1997. The proteasome: a macromolecular assembly designated to confine proteolysis to a nanocompartment. Biol. Chem. 378, 121–130.

Bensimon, D., 1996. Force: a new structural control parameter? Curr. Biol. 4, 885–889.

Binnig, G., Quate, C.F., Gerber, C., 1986. Atomic force microscope. Phys. Rev. Lett. 56, 930.

Bork, P., Holm, L., Sander, C., 1994. The immunoglobulin fold. Structural classification, sequence patterns and common core. J. Mol. Biol. 242, 309–320.

Brockwell, D.J., Smith, D.A., Radford, S.E., 2000. Protein folding mechanisms: new methods and emerging ideas. Curr. Opin. Str. Biol. 10, 16–25.

Brzeska, H., Venyaminov, S.V., Gravarek, Z., Drabikowski, W., 1983. Comparative studies on thermostability of calmodulin, skeletal muscle troponin C and their triptic fragments. FEBS Lett. 153, 169–173.

Buijs, J., Norde, W., Lichtenbelt, J.W.T., 1996. Changes in the secondary structure of adsorbed IgG and F(ab′)(2) studied by FTIR spectroscopy. Langmuir 12, 1605–1613.

Burnham, N.A., Colton, R.J., 1989. Measuring the nanomechanical properties and surface forces of materials using an atomic force microscope. J. Vac. Sci. Technol. A7, 2906–2913.

Bustamante, C., Rivetti, C., Keller, D.J., 1997. Scanning force microscopy under aqueous solutions. Curr. Opin. Str. Biol. 7, 709–716.

Bustamante, C., Smith, S.B., Liphardt, J., Smith, D., 2000. Single-molecule studies of DNA mechanics. Curr. Opin. Str. Biol. 10, 279–285.

Carrion-Vazquez, M., Oberhauser, A.F., Fowler, S.B., Marszalek, P.E., Broedel, S.E., Clarke, J., Fernandez, J.M., 1999a. Mechanical and chemical unfolding of a single protein: A comparison. Proc. Natl. Acad. Sci. USA 96, 3694–3699.

Carrion-Vazquez, M., Marszalek, P.E., Oberhauser, A.F., Fernandez, J.M., 1999b. Atomic force microscopy captures length phenotypes in single proteins. Proc. Natl. Acad. Sci. USA. 96, 11288–11292.

Casasnovas, J.M., Stehle, T., Liu, J.H., Wang, J.H., Springer, T.A., 1998. A dimeric crystal structure for the N-terminal two domains of intercellular adhesion molecule-1. Proc. Nat. Acad. Sci. USA 95, 4134–4139.

Chicurel, M.E., Chen, C.S., Ingber, D.E., 1998. Cellular control lies in the balance of forces. Curr. Opin. Cell. Biol. 10, 232–239.

Chothia, C., Jones, E.Y., 1997. The molecular structure of cell adhesion molecules. Annu. Rev. Biochem. 66, 823–862.

Clarke, J., Cota, E., Fowler, S.B., Hamill, S.J., 1999. Folding studies of immunoglobulin-like beta-sandwich proteins suggest that they share a common folding pathway. Str. Fold. Des. 7, 1145–1153.

Czajkowsky, D.M., Shao, Z., 1998. Submolecular resolution of single macromolecules with atomic force microscopy. FEBS Lett. 430, 51–54.

DeSilva, T.M., Harper, S.L., Kotula, L., Hensley, P., Curtis, P.J., Otvos Jr., L., Speicher, D.W., 1997. Physical properties of a single-motif erythrocyte spectrin peptide: a highly stable independently folding unit. Biochemistry 36, 3991–3997.

Engel, A., Gaub, H.E., Muller, D.J., 1999. Atomic force microscopy: a forceful way with single molecules. Curr. Biol. 9, R133–R136.

Erickson, H.P., 1994. Reversible unfolding of fibronectin type III and immunoglobulin domains provides the structural basis for stretch and elasticity of titin and fibronectin. Proc. Natl. Acad. Sci. USA 91, 10114–10118.
Erickson, H.P., 1997. Stretching single protein molecules: titin is a weird spring. Science 276, 1090–1092.
Evans, E., Ritchie, K., 1997. Dynamic strength of molecular adhesion bonds. Biophys. J. 72, 1541–1555.
Fisher, T.E., Marszalek, P.E, Oberhauser, A.F., Carrion-Vazquez, M., Fernandez, J.M., 1999a. The micro-mechanics of single molecules studied with atomic force microscopy. J. Physiol. -London 520, 5–14.
Fisher, T.E., Oberhauser, A.F., Carrion-Vazquez, M., Marszalek, P.E., Fernandez, J.M., 1999b. The study of protein mechanics with the atomic force microscope. Trends Biochem. Sci. 24, 379–384.
Fisher, T.E., Marszalek, P.E., Fernandez, J.M., 2000a. Stretching single molecules into novel conformations using the atomic force microscope. Nat. Struct. Biol. 7, 719–724.
Fisher, T.E., Carrion-Vazquez, M., Oberhauser, A.F., Li, H., Marszalek, P.E., Fernandez, J.M., 2000b. Single molecule force spectroscopy of modular proteins in the nervous system. Neuron 27, 435–446.
Florin, E.L., Moy, V.T., Gaub, H.E., 1994. Adhesive forces between individual ligand-receptor pairs. Science 264, 415–417.
Gerstein, M., Levitt, M., 1997. A structural census of the current population of protein sequences. Proc. Natl. Acad. Sci. USA 94, 11911–11916.
Glick, B.S., 1995. Can Hsp70 proteins act as force-generating motors?. Cell 80, 11–14.
Gopalakrishna, R., Anderson, W.B., 1982. Ca^{2+}-induced hydrophobic site on calmodulin: application for purification of calmodulin by phenyl-sepharose affinity chromatography. Biochem. Biophys. Res. Commun. 104, 830–836.
Graham, G.J., Maio, J.J., 1992. A rapid and reliable method to create tandem arrays of short DNA sequences. BioTechniques 13, 780–789.
Granzier, H., Kellermayer, M., Helmes, M., Trombitas, K., 1997. Titin elasticity and mechanism of passive force development in rat cardiac myocytes probed by thin-filament extraction. Biophys. J. 73, 2043–2053.
Harpaz, Y., Chothia, C., 1994. Many of the immunoglobulin superfamily domains in cell adhesion molecules and surface receptors belong to a new structural set which is close to that containing variable domains. J. Mol. Biol. 238, 528–539.
Hartley, J.L., Gregori, T.J., 1981. Cloning multiple copies of a DNA segment. Gene 13, 347–353.
Hayashi, N., Matsubara, M., Takasaki, A., Titani, K., Taniguchi, H., 1998. An expression system of rat calmodulin using T7 phage promoter in Escherichia coli. Prot. Express. Purif. 12, 25–28.
Hlady, V., Buijs, J., 1998. Local and global optical spectroscopic probes of adsorbed proteins. In: Malmsten, M. (Ed.), Biopolymers at Interfaces. Dekker, New York, pp. 181–220.
Horowits, R., 1999. The physiological role of titin in striated muscle. Rev. Physiol. Biochem. Pharmacol. 138, 57–96.
Hynes, R.O., 1999. The dynamic dialogue between cells and matrices: implications of fibronectin's elasticity. Proc. Natl. Acad. Sci. USA 96, 2588–2590.
Improta, S., Politou, A.S., Pastore, A., 1996. Immunoglobulin-like modules from titin I-band: extensible components of muscle elasticity. Structure 4, 323–337.
Improta, S., Krueger, J.K., Gautel, M., Atkinson, R.A., Lefevre, J.F., Moulton, S., Trewhella, J., Pastore, A., 1998. The assembly of immunoglobulin-like modules in titin: implications for muscle elasticity. J. Mol. Biol. 284, 761–777.
Jackson, S.E., 1998. How do small single-domain proteins fold? Fold. Des. 3, R81–R91.
Janshoff, A., Neitzert, M., Oberdörfer, Y., Fuchs, H., 2000. Force spectroscopy of molecular systems — single molecule spectroscopy of polymers and biomolecules. Augew. Chem. Int. Ed. 39, 3212–3237.
Kellermayer, M.S., Smith, S.B., Granzier, H.L., Bustamante, C., 1997. Folding-unfolding transitions in single titin molecules characterized with laser tweezers. Science 276, 1112–1116.
Lee, G.U., Chrisey, L.A., Colton, R.J., 1994. Direct measurement of the forces between complementary strands of DNA. Science 266, 771–773.
Li, H., Oberhauser, A.F., Fowler, S.B., Clarke, J., Fernandez, J.M., 2000. Atomic force microscopy reveals the mechanical design of a modular protein. Proc. Natl. Acad. Sci. USA 97, 6527–6531.
Li, H., Carrion-Vazquez, M., Oberhauser, A.F., Marszalek, P.E., Fernandez, J.M., in press. Point mutations alter the mechanical stability of immunoglobulin modules. Nature Str. Biol.
Linke, W.A., 2000. Stretching molecular springs: elasticity of titin filaments in vertebrate striated muscle. Histol. Histopathol. 15, 799–811.

Linke, W.A., Ivemayer, M., Olivier, N., Kolmerer, B., Ruegg, J.C., Labeit, S., 1996. Towards a molecular understanding of the elasticity of titin. J. Mol. Biol. 261, 62–71.

Linke, W.A., Rudy, D.E., Centner, T., Gautel, M., Witt, C., Labeit, S., Gregorio, C.C., 1999. I-band titin in cardiac muscle is a three-element molecular spring and is critical for maintaining thin filament structure. J. Cell Biol. 146, 631–644.

Lu, H., Isralewitz, B., Krammer, A., Vogel, V., Schulten, K., 1998. Unfolding of titin immunoglobulin domains by steered molecular dynamics simulation. Biophys. J. 75, 662–671.

Lu, H., Schulten, K., 1999. Steered molecular dynamics simulations of force-induced protein domain unfolding. Proteins. 35, 453–463.

Ludwig, M., Rief, M., Schmidt, L., Li, H., Oesterhelt, F., Gautel, M., Gaub, H.E., 1999. AFM, a tool for single-molecule experiments. Appl. Phys. A 68, 173–176.

Marko, J.F., Siggia, E.D., 1995. Stretching DNA. Macromolecules 28, 8759–8770.

Marszalek, P.E., Pang Y.P., Li, H., El Yazal, J., Oberhauser, A.F., Fernandez, J.M., 1999a. Atomic levers control pyranose ring conformations. Proc. Natl.Acad. Sci. USA 96, 7894–7898.

Marszalek, P.E., Lu, H., Li, H., Carrion-Vazquez, M., Oberhauser, A.F., Shulten, K., Fernandez, J.M., 1999b. Mechanical unfolding intermediates in titin modules. Nature 402, 100–103.

Marszalek, P.E., Oberhauser, A.F., Pang, Y.P., Fernandez, J.M., 1998. Polysaccharide elasticity governed by chair-boat transitions of the glucopyranose ring. Nature 396, 661–664.

Minajeva, A., Ivemeyer, M., Fernandez, J.M., Linke, W.A., Unfolding of titin domains explains the viscoelastic behavior of skeletal myofibrils. Submitted for publication.

Murzin, A.G., Brenner, S.E., Hubbard, T., Clothia, C., 1995. scop: a structural classification of proteins database for the investigation of sequences and structures. J. Mol. Biol. 247, 536–540.

Oberhauser, A.F., Marszalek, P.E., Erickson, H.P., Fernandez, J.M., 1998. The molecular elasticity of tenascin, an extracellular matrix protein. Nature 393, 181–185.

Oberhauser, A.F., Marszalek, P.E., Carrión-Vázquez, M., Fernández, J.M., 1999. Single protein misfolding events captured by atomic force microscopy. Nat. Struct. Biol. 6, 1025–1028.

Oesterhelt, F., Oesterhelt, D., Pfeifer, M., Engel, A., Gaub, H.E., Miller, D.J., 2000. Unfolding pathways of individual bacteriorhodopsius. Science 288, 143–146.

Ohashi, T., Kiehart, D.P., Erickson, H.P., 1999. Dynamics and elasticity of the fibronectin matrix in living cell culture visualized by fibronectin-green fluorescent protein. Proc. Natl. Acad. Sci. USA. 96, 2153–2158.

Perin, M.S., Fried, V.A., Mignery, G.A., Jahn, R., Sudhof, T.C., 1990. Phospholipid binding by a synaptic vesicle protein homologous to the regulatory region of protein kinase C. Nature 345, 260–263.

Pfanner, N., Meijer, M., 1995. Pulling in the proteins. Curr. Biol. 5, 132–135.

Plaxco, K.W., Simons, K.T., Baker, D., 1998. Contact order, transition state placement and the refolding rates of single domain proteins. J. Mol. Biol. 277, 985–994.

Politou, A.S., Gautel, M., Pfuhl, M., Labeit, S., Pastore, A., 1994a. Immunoglobulin-type domains of titin: same fold, different stability?. Biochemistry 33, 4730–4737.

Politou, A.S., Gautel, M., Joseph, C., Pastore, A., 1994b. Immunoglobulin-like domains of titin are stabilized by amino-terminal extension. FEBS Lett. 352, 27–31.

Politou, A.S., Thomas, D.J., Pastore, A., 1995. The folding and stability of titin immunoglobulin-like modules, with implications for the mechanism of elasticity. Biophys. J. 69, 2601–2610.

Politou, A.S., Gautel, M., Improta, S., Bangelista, L., Pastore, A., 1996. The elastic I-band region of titin is assembled by weakly interacting Ig-like domains. J. Mol. Biol. 255, 604–616.

Rief, M., Gautel, M., Oesterhelt, F., Fernandez, J.M., Gaub, H.E., 1997a. Reversible unfolding of individual titin immunoglobulin domains by AFM. Science 276, 1109–1112.

Rief, M., Gautel, M., Schemmel, A., Gaub, H.E., 1998. The mechanical stability of immunoglobulin and fibronectin III domains in the muscle protein titin measured by atomic force microscopy. Biophys. J. 75, 3008–3014.

Rief, M., Oesterhelt, F., Heymann, B., Gaub, H.E., 1997b. Single molecule force spectroscopy on polysaccharides by atomic force microscopy. Science 275, 1295–1297.

Rief, M., Pascual, J., Saraste, M., Gaub, H.E., 1999. Single molecule force spectroscopy of spectrin repeats: low unfolding forces in helix bundles. J. Mol. Biol. 286, 553–561.

Rothman, J.E., Kornberg, R.D., 1986. An unfolding story of protein translocation. Nature 322, 209–210.
Sambrook, J., Fritsch, E.F., Maniatis, T., 1989. Molecular Cloning: A Laboratory Manual, 2nd Edition. Cold Spring Harbor Laboratory Press, Cold Spring Harbor, NY.
Shao, X., Davletov, B.A., Sutton, R.B., Sudhof, T.C., Rizo, J., 1996. Bipartite Ca^{2+}-binding motif in C_2 domains of synaptotagmin and protein kinase C. Science 273, 248–251.
Shaub, A., 1999. Unraveling the extracellular matrix. Nature Cell Biol. 1, E173–E175.
Shtilerman, M., Lorimer, G.H., Englander, S.W., 1999. Chaperonin function: folding by forced unfolding. Science 284, 822–825.
Smith, B.L., Schaffer, T.E., Viani, M., Thompson, J.B., Frederick, N.A., Kindt, J., Belcher, A., Stucky, G.D., Morse, D.E., Hansma, P.K., 1999. Molecular mechanistic origin of the toughness of natural adhesives, fibres and composites. Nature 399, 761–763.
Strick, T.R., Allemand, J.-F., Bensimon, D., Croquette, V., 2000. Stress-induced structural transitions in DNA and proteins. Annu. Rev. Biophys. Biomed. Struct. 29, 523–543.
Studier, F.W., Rosemberg, A.H., Dunn, J.J., Dubendorff, J.W., 1990. Use of T7 RNA polymerase to direct expression of cloned genes. Meth. Enzymol. 185, 60–89.
Sudhof, T.C., Rizo, J., 1996. Synaptotagmins: C2-domain proteins that regulate membrane traffic. Neuron 17, 379–388.
Sutton, R.B., Davletov, B.A., Berghuis, A.M., Sudhof, T.C., Sprang, S.R., 1995. Structure of the first C2 domain of synaptotagmin I: a novel Ca^{2+}-phospholipid binding fold. Cell 80, 929–938.
Trinick, J., Tskhovrebova, L., 1999. Titin: a molecular control freak. Trends Cell Biol. 9, 377–380.
Wallace, R.W., Tallant, E.A., Cheung, W.Y., 1980. Assay, preparation, and properties of calmodulin. In: Calcium and Cell Function, Vol. 1. Academic Press, New York, pp. 13–40.
Witt, C.C., Olivieri, N., Centner, T., Kolmerer, B., Millevoi, S., Morell, J., Labeit, D., Labeit, S., Jockusch, Pastore, A., 1998. A survey of the primary structure and the interspecies conservation of I-band titin's elastic elements in vertebrates. J. Struct. Biol. 122, 206–215.
Yang, G., Cecconi, C., Baase, W.A., Vetter, I.R., Breyer, W.A., Haack, J.A., Matthews, B.W., Dahlquist, F.W., Bustamante, C., 2000. Solid-state synthesis and mechanical unfolding of polymers of T4 lysozyme. Proc. Natl. Acad. Sci. USA 97, 139–144.